Pathway to fully-renewable biobased polyesters derived from HMF and phenols

Journal:	*Polymer Chemistry*
Manuscript ID	PY-ART-10-2021-001441.R1
Article Type:	Paper
Date Submitted by the Author:	20-Jan-2022
Complete List of Authors:	Tavana, Jalal; University of Maine, Chemical and Biomedical Engineering Faysal, Atik; University of Maine, Chemistry Vithanage, Anushka; University of Maine, Chemistry Gramlich, William; University of Maine, Chemistry Schwartz, Thomas; University of Maine, Chemical and Biological Engineering

SCHOLARONE™
Manuscripts

Journal Name

Pathway to fully-renewable biobased polyesters derived from HMF and phenols[†]

Jalal Tavana,[a,c‡] Atik Faysal,[b,c‡] Anushka Vithanage,[b,c] William M. Gramlich,[*b,c,d] and Thomas J. Schwartz[*a,c,e]

Building on previous work where 5-hydroxymethylfurfural (HMF) was selectively functionalized by etherification with phenols, we demonstrated that the oxidized versions of these HMF ethers can be converted to functionalized δ-hexalactones (FDHLs) that can subsequently undergo ring-opening polymerization (ROP) to form polyesters. The key step in FDHL production is Ru-catalyzed selective hydrogenolysis of the C–O bond of functionalized-2-furan carboxylic acids (FFCAs). We found that the combination of TiO_2 support and a polar, aprotic solvent leads to high selectivity towards the lactone product. Under the optimized conditions, we achieved a 60% yield of FDHL at 150 °C with 1.5% Ru/TiO_2 in 1,4-dioxane using 5-phenoxy-2-furan carboxylic acid as a model reactant. ROP of six-membered lactone monomers bearing either a methoxy (MDHL) or a phenolic (PDHL) pendant group resulted in polymers ranging from 5 to 30 kg mol^{-1} with narrow dispersity. The polymerizations were carried out at room temperature using diphenyl phosphate (DPP) and triazabicyclodecene (TBD) as organocatalysts. Typical equilibrium polymerization behavior was observed at room temperature, and the reaction was observed to be pseudo-first order with respect to monomer concentration in solution. Poly(PDHL) had a significantly higher glass transition temperature (6 °C) than unsubstituted poly(valerolactone) due to the presence of the bulky phenolic group off the polymer backbone.

1 Introduction

Petroleum-based thermoplastics are ubiquitous in our daily life, but the widespread use of these nondegradable plastics has created a waste management problem that has left a significant mark on the environment.[1,2] Sustainable polymers produced from lignocellulosic biomass have the potential to reduce the environmental impact of commercial plastics while also offering significant performance benefits relative to petrochemical-derived macromolecules.[3] Cellulose, hemicellulose, and lignin are the three primary components of lignocellulosic biomass, which can be transformed into platform chemicals like 5-hydroxymethylfurfural (HMF)[4–6] and lignin-derived phenols[7–10] that in turn can be used as building blocks for the production of various bio-based monomers.[11,12]

Many polymerization processes require α,ω-functionalized monomers, with diols, dicarboxylic acids, or lactones being commonly employed.[13] However, the complex structure of bio-based feedstocks complicates the direct synthesis of such monomers;[14] therefore, a platform chemical approach is often applied. For example, diols are important monomers for polyester production, and several groups have reported the synthesis of diols using furfural as a platform molecule.[15–21] Similarly, HMF is often suggested as a suitable platform for monomer synthesis,[22–24] with 2,5-furandicarboxylic acid (FDCA) reported to be a functional replacement for terephthalic acid used in the production of plastic soda bottles.[25–27] For all of these examples, the carbon is originally derived from biomass sugars, but direct activation of the nearly identical C-O bonds in sugar molecules is difficult to achieve with high selectivity. Success in each case lies in the use of platform chemicals (e.g., furfural, HMF, or levoglucosenone) that have been partially de-functionalized to provide molecular "handles" that can be selectively upgraded. HMF is particularly attractive in this regard because it possesses both a hydroxyl group and an aldehyde that can undergo reactions independently. Illustrat-

[a] Department of Chemical & Biomedical Engineering, University of Maine, Orono, ME, USA. Fax: 207-581-2323; Tel: 207-581-2294; E-mail: thomas.schwartz@maine.edu

[b] Department of Chemistry, University of Maine, Orono, ME, USA. Fax: 207-581-1191; Tel: 207-581-1173; E-mail: william.gramlich@maine.edu
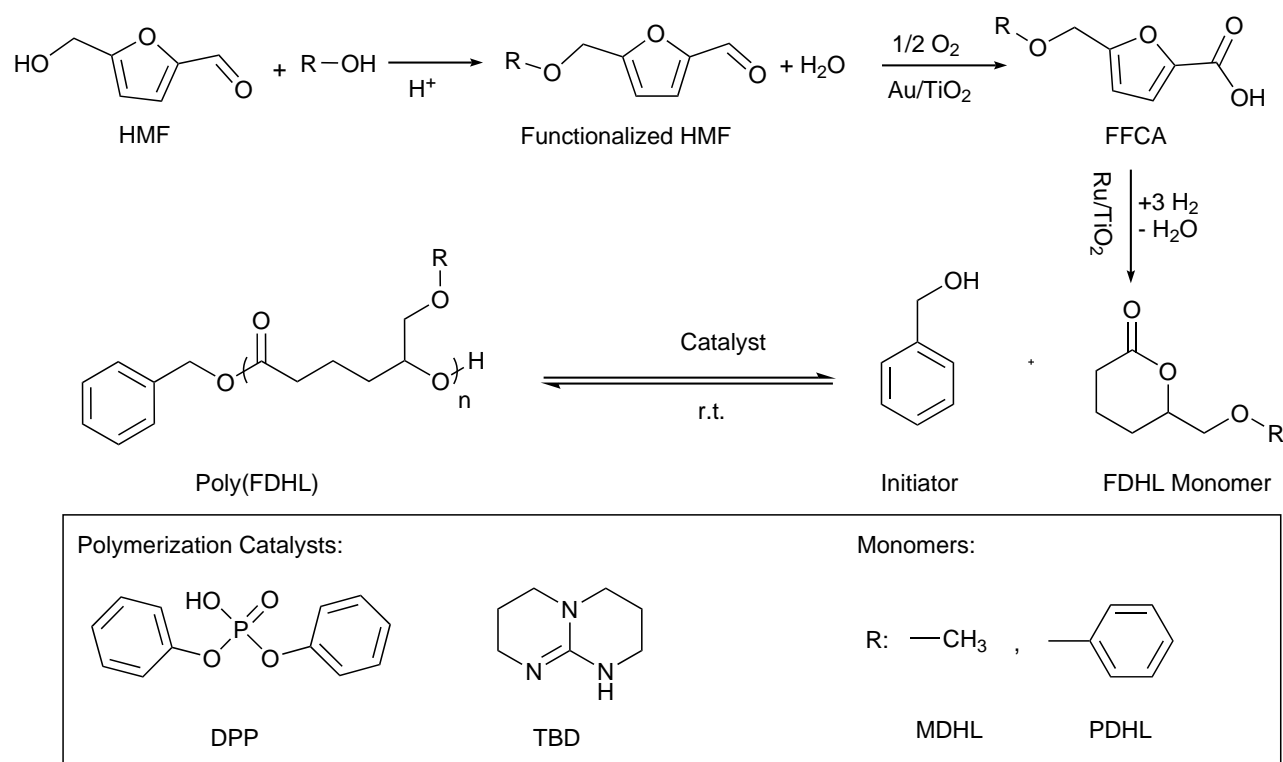
[c] Forest Bioproducts Research Institute, University of Maine, Orono, ME, USA.

[d] Advanced Structures and Composites Center, University of Maine, Orono, ME, USA.

[e] Frontier Institute for Research in Sensor Technology, University of Maine, Orono, ME, USA.

‡ These authors contributed equally to this work.

Scheme 1 Catalytic upgrading of HMF to functionalized δ-hexalactone (FDHL) followed by ring opening polymerization (ROP) to yield polyFDHLs.

ing the ability of HMF to undergo selective upgrading, we have recently shown that zeolite catalysts can be used to etherify the hydroxyl group in HMF with a variety of alcohols, including phenols that can be obtained from lignin,[28] which opens the door to the production of HMF-based polymers with tunable pendant groups.

Current bio-based thermoplastics such as poly(lactic acid) (PLA) are commercially relevant, but they cannot replace all petroleum-based thermoplastics because they do not have tunable glass transition temperatures (T_g), toughness, and barrier properties.[29–31] Thus, new polymers from inexpensive bio-derivable starting materials are an ongoing research interest. Aliphatic polyesters with minimal modifications off the backbone (*e.g.*, short alkyl chains) do not produce the variety of T_gs necessary for all applications.[32] Poly(δ-valerolactones) from renewable resources with selectable bio-derivable pendant groups have the potential to overcome these limitations. By introducing different pendant functional groups, we can tune the properties and expand the versatility of aliphatic polyesters. Rotational barriers of the polymer backbone can be increased by adding bulky groups to the polymer chain, which results in higher T_g, similar to how polylactide has been modified by introducing bulky side groups.[33–36] Lignin is the second most abundant natural polymer after cellulose and a renewable source of aromatic compounds, like phenol and substituted phenols,[37] and lignin pendant groups have been incorporated in polyacrylates to significantly increase the glass transition temperature.[36,38] Similarly, we hypothesize that incorporating these lignin-derived aromatic molecules as pendant groups in aliphatic polyesters can be used to not only increase but also to tune their glass transition temperature.

The synthesis and ring-opening polymerization (ROP) of functionalized lactones is a powerful strategy to generate functionalized polyesters[39] and their well-known depolymerization methods such as ester hydrolysis and transesterification could provide a recyclable methodology to mitigate concerns about end-of-life plastic disposal.[40] Six membered lactones can be polymerized using organocatalysts and their low ring strain facilitates recycling through depolymerization back to monomer by heating above the ceiling temperature.[41,42] However, in general polymerized six-membered lactones have low T_g (around -70 to -60 °C), and incorporating pendant alkyl groups at the δ-position of δ-valerolactone (DVL) has not substantially changed the T_g of the corresponding polyester.[43] DVL derivatives bearing bulkier pendant groups have not been studied thoroughly due to the limited availability of diverse monomers. To our knowledge, no reports exist of a systematic method to yield a range of higher T_g values by introducing different pendant groups off the fixed polymer backbone, while maintaining a potentially fully renewable origin.

In this work, we seek to capitalize on our recent observation that HMF can be selectively functionalized with lignin-based pendant groups[28] to create lactone monomers that can undergo ROP. The process is shown in Scheme 1, with the first step being oxidation of the aldehyde group in HMF, which leads to a functionalized furan carboxylic acid (FFCA). This step is directly analogous to oxidation of furfural to furan-2-carboxylic acid (FCA)[44–46] and of HMF to FDCA.[25–27] We hypothesize that, in the second step in the process, such FFCAs can be converted to functionalized δ-hexalactones (FDHLs) using bifunctional catalysts that

contain both acid sites and hydrogenating metals to catalyze saturation and C-O hydrogenolysis of the furan ring, leading to an α-ωhydroxyacid that would undergo rapid lactonization. Saturation of furan rings is known to occur over hydrogenation catalysts including Pd,[47] Pt,[48] Ru,[49] and C-O hydrogenolysis of tetrahydrofuran rings and related species is also well-documented over bifunctional catalysts[50] including RhRe/C,[51,52] PtRe/C,[53] and PtMo/C.[54] Importantly, this approach introduces a selectivity challenge because reduction of the carboxyl group in FFCA is undesirable, whereas this has not been a problem for previous work focused on tetrahydrofuran rings. Recent reports from Tomishige's group,[13,55,56] have demonstrated that hydroxy acids can be produced directly from FCA using a range of bimetallic catalysts (*e.g.*, Rh–WO$_x$/SiO$_2$, Pt–MoO$_x$/TiO$_2$). As expected, these catalysts saturate the furan ring, leading to production of tetrahydrofurancarboxylic acid (THFCA) as a primary product, but these authors also observe primary C-O cleavage at the α-position of FCA, leading to other primary products such as valeric acid (VA) and 5-hydroxyvaleric acid (5-HVA). Under acidic conditions, 5-HVA lactonizes to yield δ-valerolactone,[57] providing a more direct route FDHLs.

To this end, we report the production of new polyesters from platform chemicals that can be obtained from cellulose and lignin following the approach shown in Scheme 1. Because we have previously shown that HMF can be coupled with alcohols via selective etherification[28] and oxidation of furanic aldehydes is well-documented to occur at nearly quantitative yield,[25] we focus here on catalytic hydrogenation and lactonization of biomass-derived FCA to DVL as a representative reaction, obtaining the highest yields of DVL reported to date. We then apply this process to synthesize two FDHL monomers using readily-available model compounds, one with a methyl pendant group and one with a phenoxy pendant group, where the latter is representative of the monomers that can be produced from a combination of HMF with lignin-derived phenols. Further, we develop an organocatalytic polymerization of model FDHL monomers containing methoxymethyl and phenoxymethyl side chains using known acidic and basic catalysts under mild conditions.[58,59] The polymerizations show equilibrium behavior as expected for six-membered lactones due to low ring strain. Differential scanning calorimetry (DSC) analysis reveals that the T_g can be controlled by incorporating different pendant groups.

2   Materials & Methods

2.1   Materials

Reagents, including 2-furancarboxlic acid (98% FCA, Acros Organics), tetrahydro-2-furancarboxylic acid (98+% THFCA, Acros Organics), 5-methyl-2-furancarboxylic acid (98% 5M2FCA, Combi-Blocks), δ-valerolactone (98% DVL, Alfa Aesar), δ-hexalactone (>99% DHL, TCI), 5-phenoxy-2-furancarboxylic acid (97% 5Ph2FCA, Maybridge), *i*-butanol, 1,4-dioxane (>99%, Alfa Aesar), methyl cyclopentanone-2-carboxylate (TCI), *p*-toluenesulfonic acid (Acros), lithium aluminum hydride (Aldrich), potassium sodium tartrate tetrahydrate (Aldrich), sodium hydride (Acros), iodomethane (Aldrich), methanesul-

fonyl chloride (Fisher), phenol (Aldrich), potassium hydroxide (Aldrich), 3-chloroperoxybenzoic acid (Acros), sodium bicarbonate (Fischer), DPP: diphenyl phosphate (Acros), TBD: 1,5,7-triazabicyclo[4.4.0]dec-5-ene (Fisher), benzyl alcohol (Aldrich), 1,4-dioxane (extra dry) (Acros), dichloromethane (anhydrous) (Acros), and N,N-dimethylformamide (anhydrous) (Aldrich) were used as received. Solid catalysts were synthesized from Ru(III) nitrosylnitrate (Ru 31.3, Alfa Aesar), and supports including Aeroxide® TiO$_2$-P25 (Evonik), γ-Al$_2$O$_3$ (Strem chemicals, 97+%), and carbon (Cabot Corporation, Vulcan XC-72). All the other solvents and reagents were used as received from commercial suppliers without further purification unless stated otherwise.

Vials and magnetic stir bars used for polymerization reactions were dried in a 100 °C oven overnight before use. DPP catalyst and PDHL monomer were dried for 24 h before use in the room temperature vacuum oven. TBD was dried overnight in the antechamber of a nitrogen glovebox and kept in the glovebox under nitrogen after received. Vials, caps, syringes, spatulas and all other materials used to set up polymerization reactions were dried in the antechamber of the glovebox overnight before use.

2.2   Heterogeneous Catalyst Synthesis

All supported Ru catalysts were prepared using incipient wetness impregnation of the relevant support. Each support was dried at 140 °C for 6 h before impregnation to desorb physisorbed H$_2$O and CO$_2$ present on the TiO$_2$ surface. An aqueous solution of Ru(NO)(NO$_3$)$_2$ was added dropwise to the dried support until the incipient wetness point was reached. Following impregnation, the wet catalyst was dried overnight at 100 °C. The dried catalyst was crushed in a mortar and sieved between 50 and 100 mesh. Reduction of the Ru was carried out in a quartz flow reactor. The catalyst was first purged in a flow of Ar to remove oxygen, after which the gas stream was switched to H$_2$ and the temperature was ramped at 1 °C min^{-1} to 400 °C, which was held for 4 h. Finally, the catalyst was cooled to ambient temperature and the reactor was back-filled with Ar. The catalyst was allowed to passivate overnight by allowing air to leak slowly into the stagnant Ar atmosphere in the reactor. Prepared catalysts were then stored in a dessicator and re-reduced *in situ* at 200 °C upon use for each experiment. This procedure was used to produce Ru/TiO$_2$ catalysts at 1.5 wt% and 5 wt% Ru loadings (1.5%Ru/TiO$_2$ and 5%Ru/TiO$_2$, respectively), a Ru/γ-Al$_2$O$_3$ catalyst at 5 wt% loading, and a Ru/C catalyst at 5% loading.

2.3   Hydrogenolysis Reaction Studies

Reaction rates and yields were measured in a 50 ml stainless steel autoclave reactor (Parr Instruments). In a typical run, 250 mg of passivated catalyst was sealed in the autoclave, which was subsequently purged thrice with N$_2$ and pressurized to 4 MPa with H$_2$. The catalyst was reduced *in situ* for 4 hours at 200 °C. Then the reactor was cooled to the target reaction temperature (typically 150 °C) and 30 ml of the feed solution (typically 5 wt% FCA in 1,4-dioxane) was injected into the reactor using an HPLC pump (ChromTech, M1 Class). The solution was mixed using a

magnetic stirrer at 500 rpm. The mixture was allowed to react for between 8 and 25 h, after which the autoclave was cooled to ambient temperature and vented. The liquid reaction products were filtered, *i*-butanol was added as an internal standard, and the mixture was analyzed by gas chromatography. Unknown products were identified by GC/MS (Agilent Technologies, 5977B MSD and 7820A GC) equipped with an HP-5-MS column (30 m × 2 mm × 0.33 μm); quantification was performed using a GC/FID (Agilent Technologies 7820A) equipped with a DBWAX column mesh (9.1 m × 2 mm × 2 μm nominal). Calibration of the GC-FID detector was performed using authentic standards and *i*-butanol as an internal standard. Conversion (X), yield (Y), and selectivity (S) were calculated as follows:

$$X[\%] = \left(1 - \frac{\text{amount of detected reactant [mM]}}{\text{amount of loaded reactant [mM]}}\right) \times 100 \quad (1)$$

$$Y[\%] = \left(\frac{\text{amount of detected products [mM]}}{\text{amount of loaded reactant [mM]}}\right) \times 100 \quad (2)$$

$$S[\%] = \left(\frac{\text{amount of detected products [mM]}}{\text{amount of reactant consumed [mM]}}\right) \times 100 \quad (3)$$

2.4 Polymerization Reaction Studies

The monomers 6-(methoxymethyl)oxan-2-one or methoxy-δ-hexalactone (MDHL) and 6-(phenoxymethyl)oxan-2-one or phenoxy-δ-hexalactone (PDHL) were synthesized for polymerization studies as described in the ESI. In a typical procedure for the bulk polymerization of MDHL, DPP catalyst (4.25 mg, 0.017 mmol) was added into liquid MDHL monomer (100 mg, 0.69 mmol) in a 4 mL vial and stirred until the catalyst was dissolved. Benzyl alcohol (1.8 μL, 0.017 mmol) was added as an initiator into the mixture and stirred for desired time at ambient temperature. After the reaction time, the polymerization was quenched by adding a significant excess of ethylamine into the mixture (to neutralize the DPP) and the pure polymer was separated by precipitation from THF in cold hexane:ether (10:1) mixture. A typical polymerization led to 88-90% conversion of MDHL.

Polymerization of phenoxy-δ-hexalactone (PDHL) proceeded as follows. Two different stock solutions of initiator and catalyst were prepared by adding 15 μL benzyl alcohol in 300 μL 1,4-dioxane and 3 mg TBD in 300 μL 1,4-dioxane separately in an N_2 filled glovebox. First, the stock solution of benzyl alcohol (5 μL, 0.0024 mmol) and then the stock solution of TBD (10 μL, 0.00072 mmol) were added using glass syringes to PDHL monomer (50 mg, 0.24 mmol) dissolved in dioxane solvent (155 μL) already in 2 mL vial with a septum. The homogenous mixture was stirred for the desired reaction time at ambient temperature. The polymerization was quenched by adding excess benzoic acid (1.76 mg, 0.014 mmol). A typical polymerization led to ca. 70% conversion of PDHL. The inactive catalyst was removed by precipitation of the pure polymer into methanol.

Polymerization kinetics measurements were carried out at ambient temperature for both MDHL and PDHL monomers. Both experiments were conducted using benzyl alcohol (BnOH) as an initiator and DPP and TBD as catalysts for MDHL and PDHL, respectively. For measurement of the MDHL polymerization kinetics, DPP catalyst (2.17 mg, 0.087 mmol) was added into liquid MDHL monomer (100 mg, 0.69 mmol) in a 4 mL vial and stirred until the catalyst was dissolved. Benzyl alcohol (0.9 μL, 0.087 mmol) was added into the mixture and stirred until reached equilibrium. Aliquots were collected over time and the DPP in these aliquots was quenched by adding deuterated chloroform containing 0.5 mg/mL of ethylamine in THF (2 M) into the mixture. Monomer conversions were determined using ^{1}H NMR spectroscopy.

For measurement of the PDHL polymerization kinetics, the stock solution of benzyl alcohol (5 μL, 0.0024 mmol) and the stock solution of TBD (10 μL, 0.00072 mmol) were added using glass syringes to PDHL monomer (50 mg, 0.24 mmol) dissolved in dioxane solvent (155 μL) in 2 mL vial with a septum. The homogenous mixture was stirred until the polymerization reached equilibrium and aliquots were collected throughout the polymerization. The aliquots were quenched by adding 30 molar excess benzoic acid and monomer conversions were determined using ^{1}H NMR spectroscopy.

For the polymerization kinetics experiments, the [Monomer]$_0$: [Initiator] and [Monomer]$_0$: [Catalyst] ratios were fixed for both monomers. Both polymerizations appeared to reach equilibrium, as indicated by a plateau in monomer conversion as a function of time. Equilibrium polymerization behavior was verified by fitting the kinetics data to Equation 4,[60] which describes monomer concentration as a function of time for an equilibrium polymerization:

$$\ln\left(\frac{[M]_0 - [M]_{eq}}{[M]_0 - [M]_t}\right) = k_{app} \cdot t \quad (4)$$

where $[M]_{eq}$ is the equilibrium monomer concentration, $[M]_0$ is the initial monomer concentration, $[M]_t$ is the monomer concentration at given a time, and k_{app} is the apparent rate constant.

For the polymerization thermodynamics experiments, the setup was the same as for the kinetics experiments, but the polymerizations were stirred in an oil bath at a range of temperatures. The temperature was varied for MDHL from 17 to 55 °C and 23 to 55 °C for PDHL. The polymerizations achieved different equilibrium monomer concentrations ($[M]_{eq}$) at different temperatures. Aliquots were collected after sufficient reaction time to reach equilibrium (*i.e.*, 48 h for MDHL and 168 h for PDHL) and quenched with either ethylamine or benzoic acid, depending on the catalyst used. The polymerization progress was tracked using ^{1}H NMR spectroscopy. To ensure the polymerizations reached equilibrium, the reactions were kept running for at least another 48 h after reaching equilibrium. To estimate enthalpy (ΔH_P°) and entropy (ΔS_P°) for the polymerization, the equilibrium monomer concentration was plotted as a function of inverse temperature and fit using a van 't Hoff analysis:

$$\ln\left(\frac{[M]_{eq}}{[M]_{ss}}\right) = \frac{\Delta H_P^\circ}{RT} - \frac{\Delta S_P^\circ}{R} \quad (5)$$

where T is the polymerization temperature, R is the ideal gas constant, and $[M]_{ss}$ is a standard state monomer concentration
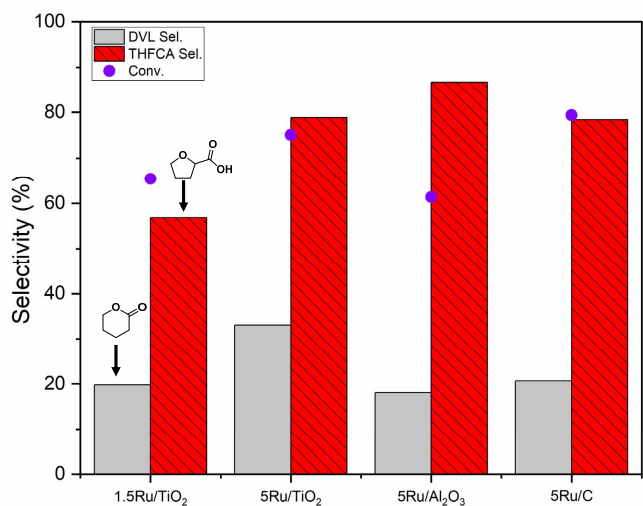
Fig. 1 Hydrogenolysis of FCA using Ru/TiO$_2$, Ru/γ-Al$_2$O$_3$, and Ru/C. Reaction conditions: FCA=400 mM, catalyst/FCA=0.03-0.53 (g:g), solvent=1,4-dioxane, 150 °C, 4 MPa H$_2$, 8 h reaction.
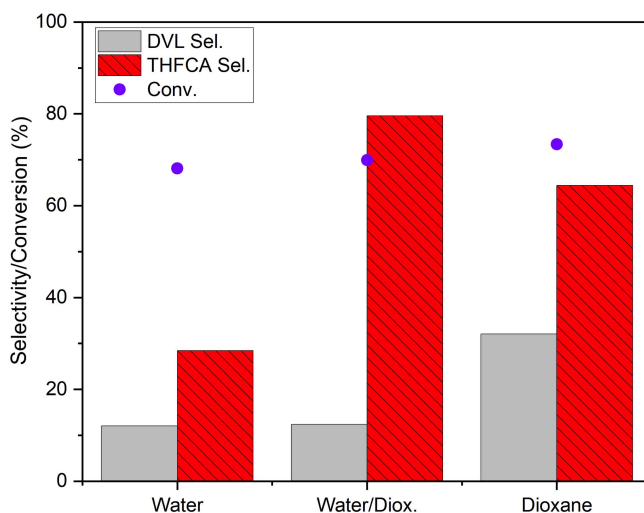

Fig. 2 Influence of solvent on FCA upgrading catalyzed by 5% Ru/TiO$_2$. No other reaction products were detected. For runs where the carbon balance does not sum to unity, the reaction products turned brown indicating the presence of polymeric degradation products (*i.e.*, humins). Reaction conditions: FCA= 200 mM , catalyst/FCA=0.67 (g:g), 4 MPa H$_2$, 150 °C, 8h.

that was set to 1 M.

2.5   Analysis of Polymer Products

^{1}H NMR and ^{13}C NMR spectra were obtained either using Varian Inova 400 MHz and Bruker Avance NEO 500 MHz NMR spectrometers using CDCl$_3$ as a solvent. Size exclusion chromatography (SEC) was conducted in dimethylformamide (DMF) containing 0.5 wt% LiBr as the mobile phase with a flow rate of 1 mL min^{-1} at 70 °C. SEC analysis was performed by three Phenogel columns (Phenomenex) in series with different pore sizes (50, 10^3, and 10^6 Å), using a refractive index detector and calibration curves from linear polystyrene standards. The T_g of different polymers was measured using a differential scanning calorimeter (DSC, TA Instruments DSC2500). Heating and cooling rates of 10 °C min^{-1} were used over a range from -65 to 80 °C using $\approx$1.5 mg sample in a heat/cool/heat experiment under an N$_2$ atmosphere. The T_g were reported from the second heating cycle and analyzed with TA TRIOS software (v5.0.0).

3   Results and Discussion

3.1   Hydrogenolysis of FCA as a Model Reactant

Model reactions were performed using FCA to produce DVL to explore how catalyst and conditions affected selectivities and yields. Several reports[13,50,55,56,61] have previously focused on FCA upgrading (Scheme 1), which can be obtained through oxidation of functionalized HMF,[27] and they suggest that hydrogenolysis of the C-O bond at the α-position requires activation of the carboxylic acid at an acid site coupled with reaction with a hydrogen adatom from a metal surface. This active site geometry (*i.e.*, an acid site adjacent to a metallic surface) is precisely that described previously for C–O hydrogenolysis during Ru/TiO$_2$-catalyzed hydrodeoxygenation.[62–64] For these catalysts, Brønsted acidic protons can be generated at the Ru-TiO$_2$ interface by spillover of hydrogen adatoms from Ru nanoparticles onto the TiO$_2$ sur-

face, and these acidic protons can participate in reaction mechanisms.[62,65,66] Accordingly, we evaluated Ru/TiO$_2$ as a catalyst for FCA upgrading, as shown in Figure 1. Notably, 5 wt% Ru/TiO$_2$ is selective not only for hydrogenation of the furan ring but also for hydrogenolysis to yield DVL, and the selectivity to DVL is higher for the TiO$_2$-supported catalyst than for Ru/C or Ru/γ-Al$_2$O$_3$, an observation that is consistent in general with the need for Brønsted acidic protons for C–O bond scission.[67,68] Because metal dispersion is generally inversely proportional to metal loading for catalysts prepared by incipient wetness impregnation, it could be possible that a catalyst containing less Ru may actually possess more Brønsted acid sites, leading to additional production of 5-HVA (and subsequently DVL); however, calculations of site time yields based on moles of Ru shows similar results between lower and higher loadings of Ru (1.22 vs 1.27 s^{-1}) which suggests that increased activity for the higher Ru-loading catalyst is likely due only to the increase in Ru loading, not a difference in Ru-TiO$_2$ interfacial area.

Recognizing that Brønsted-acid-catalyzed reactions, including the upgrading of FCA over bifunctional catalysts,[55,69] are often affected by the presence of water in the reaction solvent[70,71] and water is generally present during biomass upgrading processes, we have evaluated the influence of water on the production of DVL from FCA. Figure 2 shows the selectivity to both DVL and THFCA as produced by 5% Ru/TiO$_2$ in pure 1,4-dioxane, pure water, and a 50 wt% mixture of water and 1,4-dioxane. The use of a polar aprotic solvent (*i.e.*, 1,4-dioxane) leads to the highest selectivities to both THFCA (64%) and DVL (32%) while the use of water leads to substantial degradation. In contrast to a previous report[55] the mixture of 1,4-dioxane and water did not lead to an average performance of the neat solvents. Interestingly, the presence of substantial amounts of water in this system does not lead
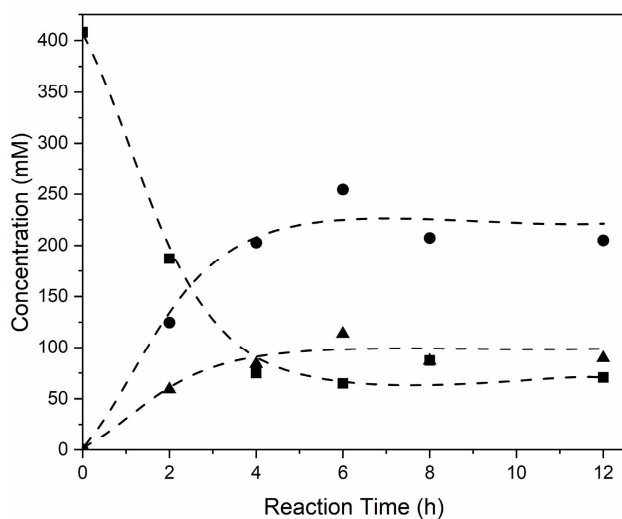
Fig. 3 Concentration profile for the conversion of FCA (■) to DVL (▲) and THFCA (●). Dashed lines serve only to guide the eye and do not represent fits to the data. Reaction conditions: FCA= 400 mM, solvent=1,4-dioxane, catalyst 5% Ru/TiO$_2$, catalyst/FCA= 0.17 (g:g), T= 150 °C, 4 MPa H$_2$.

to increases in selectivity to DVL. It has been previously shown by Nelson et al.[62] that the presence of water facilitates C–O hydrogenolysis by inhibiting oxygen vacancy creation at the Ru-TiO$_2$ interface, thereby facilitating the formation of acidic protons during hydrogen spillover. While we assume the same phenomenon will occur here, clearly these protons do not have a significant positive effect on the reaction, suggesting the mechanism of DVL formation over Ru/TiO$_2$ is distinct from that of C–O hydrogenolysis of non-acidic furans and alcohols by bimetallic nanoparticles as described by Dumesic et al.,[51,52] Neurock et al.,[72] and Davis et al.[53,73] Instead, the mechanism proposed by Tomishige et al. for FCA conversion,[13,55,56] which involves competitive formation of DVL and THFCA, appears to be operative here.

Tomishige and coworkers have studied the reduction of FCA over a variety of catalysts,[13,55,56] and they propose that C–O bond scission at the 2-position can occur even if the furan ring has not first been saturated. Notably, they evaluated hydrogenolysis of THFCA but obtained only ca. 1% DVL yield at 18% conversion using Pt-MoO$_x$/TiO$_2$ as a catalyst. Similarly, we obtained 10% yield of DVL at 20% THFCA conversion using 5% Ru/TiO$_2$ as a catalyst (Table 2 Entry 13). Figure 3 shows the concentration profile for FCA upgrading using 5% Ru/TiO$_2$. Notably, both DVL and THFCA are produced at short reaction times, and neither is consumed as the reaction proceeds, indicating that both DVL and FCA are primary reaction products (Figure 3). The reaction appears to stop after 6 h, which could be the result of either an equilibrium limitation or catalyst deactivation. The literature reports results of FCA conversion approaching 100%, indicating that equilibrium limitations should not be significant here; indeed, as shown in the ESI (Figure S1), the equilibrium constants for production of both DVL and THFCA from FCA are highly favorable. Consequently, it seems likely that this catalyst undergoes deactivation above 85% FCA conversion; thermogravimetric analysis (TGA) suggests this

deactivation is due to some process other than carbon deposition (*vide infra*). A full analysis of the mechanism of catalyst deactivation is beyond the scope of the present work, although this is the subject of ongoing investigations.

3.2 Hydrogenolysis of Substituted FCAs

While hydrogenolysis of FCA is a convenient model reaction, with precedent in the literature that is useful for comparison purposes, poly-DVL has a low T_g that is useful in only a few applications. Consequently, we evaluated the potential to apply the same catalyst system to the conversion of substituted furan carboxylic acids, which would allow for the eventual application of selectively etherified HMF as a source of monomers (following aldehyde oxidation). However, owing to the small number of applications of FFCAs, there are few commercially available examples to study at present. Consequently, for our preliminary work, we studied 5-methyl-2-furancarboxylic acid (5MFCA) because it is an inexpensive, readily available substrate that has a similar structure to our ultimate target, phenoxymethyl-furan carboxylic acid (PFCA). Based on FCA hydrogenolysis reactions, we anticipated that 5% Ru/TiO$_2$ would be more active than 1.5% Ru/TiO$_2$ under similar reaction conditions; however, in the case of 5MFCA we observed the opposite to be true (Table 1, Entries 2 and 3). TGA in an oxygen atmosphere performed on the spent catalyst confirms that the catalyst did not deactivate due to carbon deposition, and the literature indicates that high conversion of 5MFCA is possible, so the reaction should not be equilibrium-limited. Therefore, we attempted to optimize the reaction conditions to maximize production of DHL. Increasing the reaction temperature leads to increased conversion of 5MFCA, but unfortunately the selectivity decreases due to degradation reactions (Table 1, Entry 5). Changing the space time by increasing the amount of catalyst and/or reaction time leads to increased conversion and improved selectivity over both catalysts (comparing Entries 1 and 2 or 3 and 5 in Table 1), although notably the increase in selectivity is only modest for the 1.5 wt% Ru/TiO$_2$ catalyst, suggesting an upper limit on the DHL yield of approx. 50%. Notably, at comparable conditions (Table 1 Entries 2 and 3), the 1.5% Ru/TiO$_2$ catalyst was more active than the 5% Ru/TiO$_2$ catalyst, which is in stark contrast to our observations for the reaction of FCA and suggests that a different mechanism, possibly involving direct production of lactone from furan, may be in play for conversion of 5MFCA.

Table 2 compares published results reported for similar reactions with our observations. At 30% yield of DVL, our observed reduction of FCA with Ru/TiO$_2$ (Entry 11) is comparable to the best yields obtained in the literature to date. Notably, though, our conversion of 5MFCA to DHL (Entry 12) over Ru/TiO$_2$ is significantly higher than other reports (*e.g.*, Entry 10). Accordingly, we evaluated these conditions for the conversion of phenol substituted FCA (5PhFCA) to produce phenoxy-δ-hexalactone (PhDHL). For a 25 h reaction at 150 °C over 1.5% Ru/TiO$_2$, we achieved 99% conversion of 5PhFCA. The presence of PhDHL in the product was confirmed by GC/MS analysis, with a yield of ca. 60% obtained by GC/FID analysis (using a linear combination of the detector response factor for phenol and DHL). To our knowl-

Table 1 Conversion of FCA to DHL using Ru/TiO$_2$ catalysts.[a]

Entry	Catalyst	Catalyst Mass (mg)	Time (h)	Temp. (°C)	Conv. (%)	DHL Sel. (%)	DHL Yield (%)
1	5% Ru/TiO$_2$	250	8	150	14	16	2
2	5% Ru/TiO$_2$	500	25	150	52	41	21
3	1.5% Ru/TiO$_2$	500	25	150	91	47	43
4	1.5% Ru/TiO$_2$	500	25	200	100	16	16
5	1.5 % Ru/TiO$_2$	1000	25	150	100	53	53

[a] Reaction conditions: 4 MPa H$_2$, 200 mM 5MFCA in 1,4-dioxane, 30 mL reaction volume.

edge, this is the first report of the production of an aromatic FDHL from fully renewable feedstocks. Moreover, because the aromatic group originates from a selective etherification (see Scheme 1), this same approach can be used to produce many different aromatic FDHLs, and the availability of such monomers opens the door to the production of a range of polymers with varying T_g, mechanical, and physical properties.

3.3 Lactone Polymerization

Parallel to the catalytic studies to produce FDHLs, six-membered lactone monomers bearing two different pendant groups, a methoxy group (MDHL) and a phenolic group (PDHL) (Scheme 1), were synthesized from commercially available methyl cyclopentanone-2-carboxylate (Figure S2) to study how the pendant groups affect polymerization and polymer properties (see ESI for monomer synthesis methods). Intermediates throughout the synthesis could be produced easily with minor impurities (see Figures S3 – S9). After the final Baeyer-Villiger oxidation step, the minor regioisomer (Figures S10 and S11) could be purified by flash chromatography to yield spectroscopically pure (^{1}H and ^{13}C NMR spectroscopy) monomers suitable for polymerization (Figures S12-S15).

The MDHL monomer (liquid) was polymerized in the bulk to ensure the highest monomer concentration, but 1,4-dioxane solvent was used to polymerize PDHL monomer (solid) to facilitate homogeneity. Both monomers were polymerized at room temperature using benzyl alcohol (BnOH) as the initiator and diphenyl phosphate (DPP) as a catalyst (Scheme 1). DPP has previously been reported to be active as an acidic organocatalyst for ROP of both unsubstituted (DVL)[74] and substituted (n-alkyl-DVL)[43] six-membered lactones. The conversion of MDHL and PDHL monomers was tracked by taking aliquots from the polymerization and analyzing them using ^{1}H NMR spectroscopy. The methylene protons of the BnOH initiator shifted from 4.7 to 5.1 ppm, confirming that both monomers were initiated by BnOH. The methine protons of MDHL (4.43 ppm) and PDHL (4.68 ppm) shifted to 5.01 and 5.17 ppm, respectively, corresponding to the lactone ring opening and the successful polymerization for both monomers (Figure S16-17).
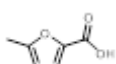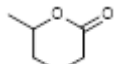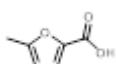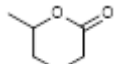
The monomer conversion of MDHL was 90% after 3 days (Table 3, Entry 1), which indicates a slower polymerization rate than unsubstituted DVL[43,60] due to steric hindrance or a decrease in ring strain by the substituents on the lactone monomers.[75,76] The number average molecular weight ($M_{n,SEC}$) of polyMDHL measured by size exclusion chromatography was 3.3 kg mol^{-1}, lower than the value expected from monomer conversion ($M_{n,expected}$). The $M_{n,SEC}$ of polyMDHLs with higher $[M]_0/[I]$ values changed

little and remained low when the polymer size was expected to increase (Table 3, Entries 1-3). This behavior suggests that either backbiting or other side reactions played a vital role in shortening the growing polymer chains. Polymerizations of MDHL without initiator yielded higher molecular weight polymers (Table S1, Runs 1-2), indicating that self-initiation likely occurred. Polymerization of PDHL catalyzed by DPP formed similar low-molecular-weight polymers with initiator (Table S2, Entries 1-4) and yielded comparatively high-molecular-weight polymers without any initiator (Table S1, Run 3), further suggesting that self-initiation occurs. Similar low molecular weight observations have been made for structurally similar hemiacetal cyclic monomers where the polymerization proceeded by both activated-monomer (AM) and active-chain-end (ACE) mechanisms while catalyzed by DPP.[77] Further studies are needed to understand the origin of low molecular weight polyFDHLs catalyzed by DPP.

To address the low molecular weights obtained using DPP, we screened TBD[78] as a catalyst. Interestingly, the MDHL monomer did not polymerize whether in bulk or solution (Table S2, Entries 5-6), yet PDHL successfully polymerized using the basic TBD catalyst in the presence of BnOH at room temperature in 1,4-dioxane. The equilibrium monomer conversion of PDHL was 70% and the $M_{n,SEC}$ of polyPDHL was close to the expected value (Table 3, Entry 4). The $M_{n,SEC}$ values could be increased by increasing $[M]_0/[I]$ for polyPDHL (Table 3, Entries 5-6). Lower catalyst loadings reduced the polymer dispersity (Table S3, Runs 1-8). Simon and Goodman reported that TBD-catalyzed ROP proceeds by either a nucleophilic or acid-base catalytic mechanism, where the nucleophilic catalytic mechanism predominates when the alcohol concentration is low compared to the catalyst loading.[79] Higher catalyst loadings relative to the alcohol may favor reaching equilibrium monomer concentration faster or the polymerization propagation through the nucleophilic mechanism instead of the acid-base mechanism, which led to the higher dispersity observed.

The polymers were purified by precipitation and the T_g was measured by DSC from the second heating cycle (Figure 4). PolyMDHL (M_n = 10 kg mol^{-1}; Table S1, Run 1) had a T_g of -44 °C, which is higher than that of unsubstituted six-membered poly(δ-valerolactone) (ca. -65 °C)[80,81] and seven-membered poly(ε-caprolactone) (-60 °C)[82] and close to that of alkyl-substituted poly(n-alkyl-DVL) (-52 °C)[43] and poly(δ-decalactone) (-51 °C).[74] The T_g for polyPDHL (M_n = 22 kg mol^{-1}) was 6 °C, a significant increase that we attribute to the presence of the bulky phenolic pendant group. This T_g is higher than those of all alkyl-substituted poly(δ-valerolactone)s (-52 °C to -50 °C) and 3-mercaptovalerolactones (-14 °C),[39] and is the highest reported

Table 2 Recent reports on reduction of FCA and MFCA to their respective lactone analogues.

Entry	Substrate	Product	Solvent	Catalyst	Conv. (%)	Sel.[a] (%)	Yield[a] (%)	Ref.
1			Methanol	Pt/Al_2O_3	99	7	7	13
2			Methanol	Pt/CeO_2	91	7	6	13
3			Methanol	Ru/C	99	1	1	13
4			Acetic Acid	Pt/Al_2O_3	55	66	36	13
5			1,4-dioxane	Pt/Al_2O_3	88	34	30	13
6			2-propanol	Pt/Al_2O_3	97	42	41	13
7			Water	$Pt-MoO_x/TiO_2$	82	10	8	58
9			Water	$Rh-WO_x/SiO_2$	62	15	9	53
10			Water	$Pt-MoO_x/TiO_2$	91	19	17	53
11[b]			1,4-dioxane	5% Ru/TiO_2	83	37	31	This Work
12[b]			1,4-dioxane	1.5 % Ru/TiO_2	100	53	53	This Work
13[b]			1,4-dioxane	5 % Ru/TiO_2	20	15	10	This Work

[a] Selectivity and yield are for the corresponding lactone product. [b] Reaction conditions: 150 °C, 4 MPa H_2, 200 mM substrate, 30 mL reaction volume, catalyst/FCA = 0.17 (g:g), 0.53 (g:g), and 0.17 (g:g) for entries 11, 12, and 13 respectively.

Table 3 Representative ROP of functionalized δ-hexalactones (FDHLs)

Monomer	Entry	$[M]_0/[I]/[C]$	Time (days)	Conv.[c] (%)	$M_{n,expected}$[d] (kg mol^{-1})	$M_{n,SEC}$[e] (kg mol^{-1})	Đ[e]
MDHL[a]	1	40/1/1	3	90	5.2	3.3	1.34
	2	80/1/1	3	88	10.2	3.7	1.33
	3	160/1/1	3	88	20.4	4.4	1.28
PDHL[b]	4	50/1/0.15	7	70	7.2	10.5	1.64
	5	100/1/0.3	10	67	14.0	22.0	1.49
	6	3001/0.9	10	50	31.0	30.0	1.59

[a] Bulk polymerization, $[M]_0$ = 6.6 M and DPP used as a catalyst. [b] 1,4-dioxane as solvent, $[M]_0$ = 1.1 M, and TBD used as a catalyst; where $[M]_0$ = Initial monomer concentration. [c] Fractional conversion measured by ^{1}H NMR spectroscopy. [d] Calculated from $[M]_0/[I] \times$ monomer conversion $\times MW$ of MDHL or PDHL. [e] Measured by SEC in THF as the mobile phase for MDHL and DMF with 0.5 wt% LiBr as the mobile phase for PDHL, using linear polystyrene standards with a refractive index detector.
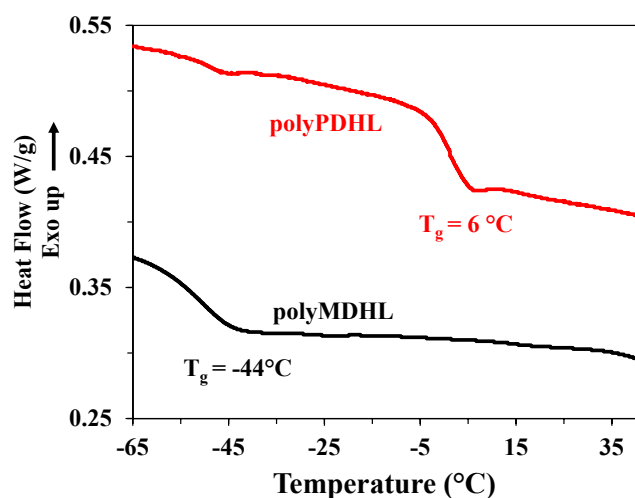
Fig. 4 DSC thermograms of polyMDHL and polyPDHL. Curves are shifted vertically to provide clarity.

for substituted VL to the best of our knowledge.[39,43,83] Neither polymer crystallized above its T_g because both were racemic mixtures and the catalysts afforded no stereochemical preference. Because the T_g increases rapidly with increasing molecular weight and plateaus at higher values,[84] we analyzed a lower molecular weight polyMDHL (M_n = 3.7 kg mol⁻¹) and found a T_g of -50 °C. No difference was observed in the T_g of polyPDHL with lower molecular weight (M_n = 7 kg mol⁻¹) (Figure S18), indicating that the T_g for polyPDHL had plateaued as a function of molecular weight. We were unable to conclude whether the T_g had reached its maximum value for polyMDHL as a function of molecular weight due to the unavailability of higher molecular weight polymers.

3.4 Polymerization Kinetics and Thermodynamics

The polymerization kinetics were analyzed for both MDHL and PDHL monomers under optimal catalyst and polymerization conditions as determined above, which demonstrated equilibrium polymerization as evidenced by plateauing conversion (Figure 5). Importantly, the optimized polymerization conditions were not identical for each monomer, so the rates of MDHL and PDHL polymerization should not be compared directly. A plot of monomer consumed as a function of reaction time is linear for MDHL and suggests that its polymerization is pseudo-zero order with respect to monomer concentration (Figure 5a – inset, see Figure S19 for deviation from first-order behavior). Schneiderman et al. found similar results for six-membered lactones where DPP-catalyzed polymerization followed pseudo zero-order kinetics when conducted in the bulk,[43] while DPP-catalyzed polymerization in dilute conditions has followed first-order kinetics.[43,60,74] Thus, our results indicate that MDHL polymerization behaves similar to other six-membered lactones in the bulk. Conversely, a semilogarithmic plot of monomer conversion as a function of reaction time for PDHL was linear, which indicates PDHL polymerization is first-order with respect to monomer concentration (Figure 5b

- inset). Martello et al. also reported that similar TBD-catalyzed δ-decalactone polymerization followed first order kinetics.[83]

The molar mass distributions were unimodal for both polymers (Figure S20), which indicated limited backbiting occurred prior to equilibrium. The molecular weight of polyMDHL and polyPDHL also linearly increased as a function of monomer conversion and the dispersity values ranged from 1.1 to 1.28 and from 1.19 to 1.6, respectively (Figure 5). This behavior is expected for controlled ROP where all chains are initiated at the same time and then propagate simultaneously. The $M_{n,SEC}$ values of polyPDHL are directly proportional to the ratio of $[M]_0/[I]$ used for polymerization, while the $M_{n,SEC}$ values for polyMDHL did not significantly change (Figure S21). The polymerization kinetics and time-dependent evolution of molecular weight for PDHL indicate that it follows controlled polymerization behavior under these conditions, while MDHL seems to deviate from the expected molecular-weight-control due to initiation events not involving BnOH. We speculate that both MDHL and PDHL can self-initiate polymerization when DPP is used as catalyst, which is the subject of ongoing research.

The thermodynamics of the ROP were examined by polymerizing MDHL (bulk, DPP catalyst) and PDHL (solution, TBD catalyst) over a range of temperatures and performing a van 't Hoff analysis to calculate the entropy and enthalpy of polymerization (Figure S22). The enthalpy of polymerizations (ΔH_P°) were -10 ± 1 kJ mol⁻¹ for MDHL and -9.4 ± 0.7 kJ mol⁻¹ for PDHL, which are close to the values reported for DVL (ca. -10 kJ mol⁻¹), but slightly lower than the values reported for δ-decalactones (-17.1 ± 0.6 kJ mol⁻¹) and other alkyl-substituted δ-lactones (-13 to -19 kJ mol⁻¹).[43,74,85] The inclusion of an ether linkage in the pendant group appears to decrease the ring strain as compared to the all-carbon pendant group of alkyl-substituted δ-lactones, which may be due to the increased rotational freedom of the ether group.[43,83] The entropies of polymerization (ΔS_P°) were -34 ± 3 J mol⁻¹ K⁻¹ for MDHL and -26 ± 2 J mol⁻¹ K⁻¹ for PDHL, whereas the value reported in the literature for DVL is around -15 J mol⁻¹ K⁻¹, which indicates that both monomers are more entropically disfavored as compared to DVL.[83] However, their entropic penalty for polymerization is less than that of alkyl-substituted DVLs (ca. -55 J mol⁻¹ K⁻¹),[43] which enables the significant conversions observed in spite of the lower ΔH_P°. The addition of a pendant group likely decreases the internal rotational freedom of a polymer chain relative to its unsubstituted parent, DVL,[43] which leads to the higher entropic penalty observed for substituted DVL monomers. However, for the ether-substituted monomers MDHL and PDHL, this entropic penalty is not as significant as for alkyl-substituted DVL monomers, presumably due to the extra degrees of freedom possible from the more freely rotating ether group. Further study is ongoing with other FDHLs to determine the origin of this lower entropic penalty. Nevertheless, these measured thermodynamic parameters indicate that FDHLs can be polymerized at room temperature and higher, achieving useful monomer conversions (i.e., >50%).
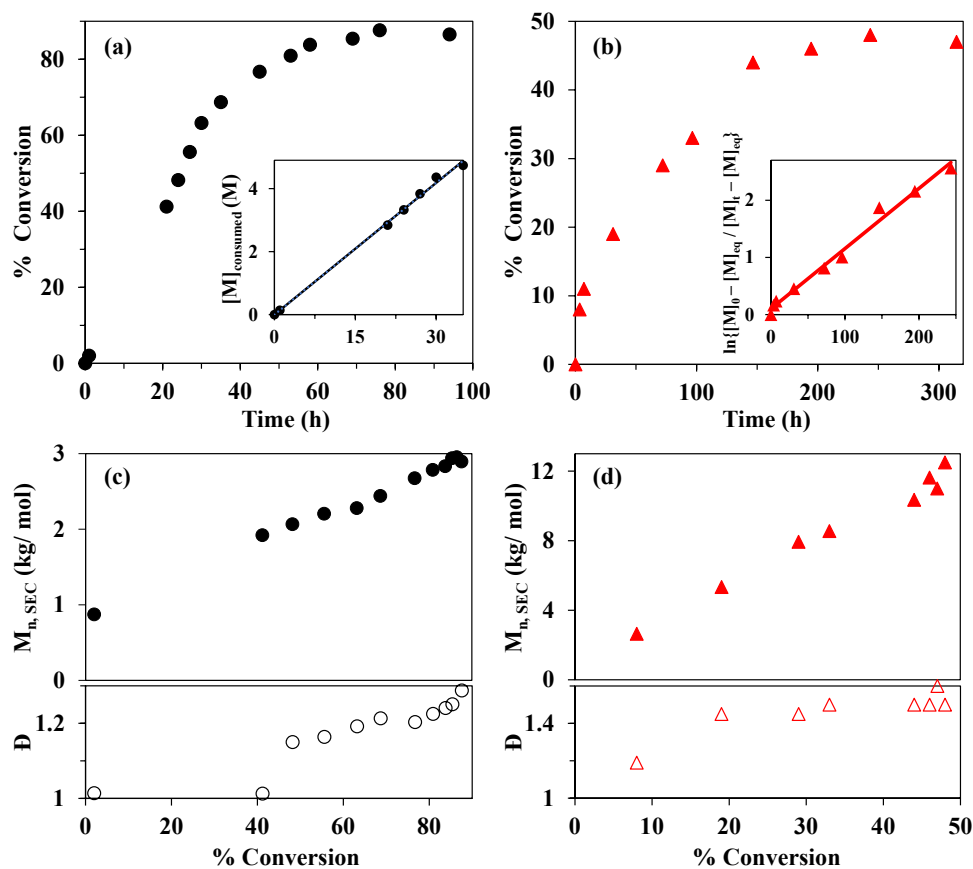
Fig. 5 a) Monomer conversion as a function of time for polyMDHL; inset shows the linearized kinetic behavior for ROP of MDHL (●) before reaching equilibrium assuming pseudo-zero order in monomer kinetics, where $[M]$consumed is the total monomer concentration consumed to form polymer ($[MDHL]_0 = 6.7$ M, $[DPP]_0 = 85$ mM, $[BnOH]_0 = 85$ mM). b) Monomer conversion as a function of time for polyPDHL; inset shows the linearized kinetic behavior for ROP of PDHL (▲) before reaching equilibrium assuming pseudo-first order in monomer kinetics, where $[M]_{eq}$ is the equilibrium monomer concentration, $[M]_0$ is the initial monomer concentration, $[M]_t$ is the monomer concentration at given a time ($[PDHL]_0 = 1.1$ M, $[TBD]_0 = 3.3$ mM, $[BnOH]_0 = 11$ mM). See ESI for description of kinetic models. c) Number average molecular weight (M_n) and dispersity (Đ) as a function of monomer conversion for poly(MDHL) (●). d) M_n and Đ as a function of monomer conversion for poly(PDHL) (▲). Both M_n and Đ measured by SEC. Ratios of $[M]_0/[I] = 80/1$ for poly(MDHL) and $[M]_0/[I] = 100/1$ for poly(PDHL) used throughout this study.

4   Conclusions

In summary, we have demonstrated a successful approach for producing polyesters with tunable glass transition temperatures using feedstocks entirely derivable from lignocellulose biomass. Lactone monomers can be synthesized with pendant group diversity starting from HMF, which can be obtained from biomass sources, and they can be functionalized with methoxy and phenolic groups in the δ-position by selective etherification of the HMF feedstock. Oxidation of the functionalized HMF leads to a functionalized furan carboxylic acid, which can be lactonized using Ru/TiO$_2$ to simultaneously reduce the C=C bonds of the furan ring while also performing C-O hydrogenolysis. Titania is more active as a catalyst support for this reaction than γ-Al$_2$O$_3$ or carbon, and the yield of lactones is higher when using a polar aprotic solvent (*i.e.*, 1,4-dioxane). Using this catalyst system, we were able to obtain 60% yield of phenoxy-δ-hexalactone, which is the highest reported to-date. Both the methoy- and phenoxy- functionalized monomers have sufficient thermodynamic driving force to polymerize in the presence of different organo-catalysts at room temperature. Ring-opening polymerization of the phenolic-functionalized lactone monomers yielded high molecular weight and low dispersity polyesters. The molecular weight of PDHL can be controlled by varying the monomer-to-initiator ratio. The introduction of a bulkier pendant group significantly increased the glass transition temperature relative the parent unsubstituted valerolactone and to a value near room temperature, yielding the highest reported T_g for a substituted δ-valerolactone. Since bulkier pendant groups led to higher T_g, ongoing work is focused on investigating the synthesis and polymerization of other functionalized lactone monomers to target T_g values greater than room temperature as well as exploring the mechanical properties of these materials.

Author Contributions

The manuscript was written through contributions of all authors. All authors have given approval to the final version of the manuscript.

Conflicts of interest

There are no conflicts to declare.

Acknowledgements

Notes and references

1 R. C. Thompson, S. H. Swan, C. J. Moore and F. S. vom Saal, *Philosophical Transactions: Biological Sciences*, 2009, **364**, 1973–1976.

2 P. L. Corcoran, C. J. Moore and K. Jazvac, *GSA Today*, 2014, **24**, 4–8.

3 R. M. O'Dea, J. A. Willie and T. H. Epps, *ACS Macro Letters*, 2020, **9**, 476–493.

4 A. H. Motagamwala, K. Huang, C. T. Maravelias and J. A. Dumesic, *Energy & Environmental Science*, 2019, **12**, 2212–2222.

5 J. M. R. Gallo, D. M. Alonso, M. A. Mellmer and J. A. Dumesic, *Green Chemistry*, 2013, **15**, 85–90.

6 J. He, M. Liu, K. Huang, T. W. Walker, C. T. Maravelias, J. A. Dumesic and G. Huber, *Green Chemistry*, 2017.

7 E. M. Anderson, M. L. Stone, R. Katahira, M. Reed, G. T. Beckham and Y. Román-Leshkov, *Joule*, 2017, **1**, 613–622.

8 W. Schutyser, T. Renders, S. Van den Bosch, S. F. Koelewijn, G. T. Beckham and B. F. Sels, *Chemical Society Reviews*, 2018, **47**, 852–908.

9 S. Jampa, A. Puente-Urbina, Z. Ma, S. Wongkasemjit, J. S. Luterbacher and J. A. van Bokhoven, *ACS Sustainable Chemistry & Engineering*, 2019, **7**, 4058–4068.

10 L. Shuai, M. T. Amiri, Y. M. Questell-Santiago, F. Héroguel, Y. Li, H. Kim, R. Meilan, C. Chapple, J. Ralph and J. S. Luterbacher, *Science*, 2016, **354**, 329.

11 T. Buntara, S. Noel, P. H. Phua, I. Melián-Cabrera, J. G. de Vries and H. J. Heeres, *Angewandte Chemie International Edition*, 2011, **50**, 7083–7087.

12 N. Yoshida, N. Kasuya, N. Haga and K. Fukuda, *Polymer Journal*, 2008, **40**, 1164–1169.

13 T. Asano, H. Takagi, Y. Nakagawa, M. Tamura and K. Tomishige, *Green Chemistry*, 2019, **21**, 6133–6145.

14 T. Schwartz, B. Shanks and J. Dumesic, *Current Opinion in Biotechnology*, 2016, **38**, 54–62.

15 X. Li, P. Jia and T. Wang, *ACS Catalysis*, 2016, **6**, 7621–7640.

16 K. Gupta, R. K. Rai and S. K. Singh, *ChemCatChem*, 2018, **10**, 2326–2349.

17 S. Chen, R. Wojcieszak, F. Dumeignil, E. Marceau and S. Royer, *Chemical Reviews*, 2018, **118**, 11023–11117.

18 F. Liu, Q. Liu, J. Xu, L. Li, Y.-T. Cui, R. Lang, L. Li, Y. Su, S. Miao, H. Sun, B. Qiao, A. Wang, F. Jérôme and T. Zhang, *Green Chemistry*, 2018, **20**, 1770–1776.

19 K. Huang, Z. J. Brentzel, K. J. Barnett, J. A. Dumesic, G. W. Huber and C. T. Maravelias, *ACS Sustainable Chemistry & Engineering*, 2017, **5**, 4699–4706.

20 S. H. Krishna, D. J. McClelland, Q. A. Rashke, J. A. Dumesic and G. W. Huber, *Green Chemistry*, 2017, **19**, 1278–1285.

21 Y. Nakagawa, M. Tamura and K. Tomishige, *ACS Catalysis*, 2013, **3**, 2655–2668.

22 T. Buntara, S. Noel, P. H. Phua, I. Melian-Cabrera, J. G. de Vries and H. J. Heeres, *Angewandte Chemie International Edition*, 2011, **50**, 7083–7087.

23 B. M. Stadler, C. Wulf, T. Werner, S. Tin and J. G. de Vries, *ACS Catalysis*, 2019, **9**, 8012–8067.

24 A. Caretto, M. Noe, M. Selva and A. Perosa, *ACS Sustainable Chemistry & Engineering*, 2014, **2**, 2131–2141.

25 A. H. Motagamwala, W. Won, C. Sener, D. M. Alonso, C. T. Maravelias and J. A. Dumesic, *Science Advances*, 2018, **4**, eaap9722.

26 S. E. Davis, L. R. Houk, E. C. Tamargo, A. K. Datye and R. J. Davis, *Catalysis Today*, 2011, **160**, 55–60.

27 S. E. Davis, B. N. Zope and R. J. Davis, *Greem Chemistry*, 2012, **14**, 143–147.

28 M. C. Allen, A. J. Hoffman, T.-w. Liu, M. S. Webber, D. Hibbitts and T. J. Schwartz, *ACS Catalysis*, 2020, **10**, 6771–6785.

29 C. R. Álvarez-Chávez, S. Edwards, R. Moure-Eraso and K. Geiser, *Journal of Cleaner Production*, 2012, **23**, 47–56.

30 S. Farah, D. G. Anderson and R. Langer, *Advanced Drug Delivery Reviews*, 2016, **107**, 367–392.

31 M. Singhvi and D. Gokhale, *RSC Advances*, 2013, **3**, 13558–13568.

32 J. A. Galbis, M. d. G. García-Martín, M. V. de Paz and E. Galbis, *Chemical Reviews*, 2016, **116**, 1600–1636.

33 H. T. H. Nguyen, P. Qi, M. Rostagno, A. Feteha and S. A. Miller, *Journal of Materials Chemistry A*, 2018, **6**, 9298–9331.

34 T. Liu, T. L. Simmons, D. A. Bohnsack, M. E. MacKay, I. Smith, Milton R. and G. L. Baker, *Macromolecules (Washington, DC, United States)*, 2007, **40**, 6040–6047.

35 G. L. Fiore, F. Jing, J. V. G. Young, C. J. Cramer and M. A. Hillmyer, *Polymer Chemistry*, 2010, **1**, 870–877.

36 K. Marcincinova-Benabdillah, M. Boustta, J. Coudane and M. Vert, *Biomacromolecules*, 2001, **2**, 1279–1284.

37 A. Gandini, *Green Chemistry*, 2011, **13**, 1061–1083.

38 A. L. Holmberg, J. F. Stanzione, R. P. Wool and T. H. Epps, *ACS Sustainable Chemistry & Engineering*, 2014, **2**, 569–573.

39 H. Kim, J. V. Olsson, J. L. Hedrick and R. M. Waymouth, *ACS Macro Letters*, 2012, **1**, 845–847.

40 A. Kumar, N. von Wolff, M. Rauch, Y.-Q. Zou, G. Shmul, Y. Ben-David, G. Leitus, L. Avram and D. Milstein, *Journal of the American Chemical Society*, 2020, **142**, 14267–14275.

41 N. E. Kamber, W. Jeong, R. M. Waymouth, R. C. Pratt, B. G. G. Lohmeijer and J. L. Hedrick, *Chemical Reviews*, 2007, **107**, 5813–5840.

42 C. Alemán, O. Betran, J. Casanovas, K. N. Houk and H. K. Hall, *The Journal of Organic Chemistry*, 2009, **74**, 6237–6244.

43 D. K. Schneiderman and M. A. Hillmyer, *Macromolecules*, 2016, **49**, 2419–2428.

44 M. Douthwaite, X. Huang, S. Iqbal, P. J. Miedziak, G. L. Brett, S. A. Kondrat, J. K. Edwards, M. Sankar, D. W. Knight, D. Bethell and G. J. Hutchings, *Catalysis Science & Technology*, 2017, **7**, 5284–5293.

45 F. Menegazzo, M. Signoretto, T. Fantinel and M. Manzoli, *Journal of Chemical Technology & Biotechnology*, 2017, **92**, 2196–2205.

46 A. Roselli, Y. Carvalho, F. Dumeignil, F. Vavani, S. Paul and R. Wojcieszak, *Catalysts*, 2020, **10**, 73.

47 S. Wang, V. Vorotnikov and D. G. Vlachos, *Green Chemistry*, 2014, **16**, 736–747.

48 H. A. Smith and J. F. Fuzek, *Journal of the American Chemical Society*, 1949, **71**, 415–419.

49 L. J. Durndell, G. Zou, W. Shangguan, A. F. Lee and K. Wilson, *ChemCatChem*, 2019, **11**, 3927–3932.

50 M. Tamura, Y. Nakagawa and K. Tomishige, *Asian Journal of Organic Chemistry*, 2020, **9**, 126–143.

51 M. Chia, B. J. O'Neill, R. Alamillo, P. J. Dietrich, F. H. Ribeiro, J. T. Miller and J. A. Dumesic, *Journal of Catalysis*, 2013, **308**, 226–236.

52 M. Chia, Y. J. Pagán-Torres, D. Hibbitts, Q. Tan, H. N. Pham, A. K. Datye, M. Neurock, R. J. Davis and J. A. Dumesic, *Journal of the American Chemical Society*, 2011, **133**, 12675–12689.

53 D. D. Falcone, J. H. Hack, A. Y. Klyushin, A. Knop-Gericke, R. Schlögl and R. J. Davis, *ACS Catalysis*, 2015, **5**, 5679–5695.

54 P. J. Dietrich, R. J. Lobo-Lapidus, T. Wu, A. Sumer, M. C. Akatay, B. R. Fingland, N. Guo, J. A. Dumesic, C. L. Marshall, E. Stach, J. Jellinek, W. N. Delgass, F. H. Ribeiro and J. T. Miller, *Topics in Catalysis*, 2012, **55**, 53–69.

55 T. Asano, Y. Nakagawa, M. Tamura and K. Tomishige, *ACS Sustainable Chemistry & Engineering*, 2019, **7**, 9601–9612.

56 T. Asano, M. Tamura, Y. Nakagawa and K. Tomishige, *ACS Sustainable Chemistry & Engineering*, 2016, **4**, 6253–6257.

57 J. Q. Bond, D. Wang, D. M. Alonso and J. A. Dumesic, *Journal of Catalysis*, 2011, **281**, 290–299.

58 A. P. Dove, *ACS Macro Letters*, 2012, **1**, 1409–1412.

59 F. Du, Y. Zheng, W. Yuan, G. Shan, Y. Bao, S. Jie and P. Pan, *Journal of Polymer Science Part A: Polymer Chemistry*, 2019, **57**, 90–100.

60 M. J. Flanders and W. M. Gramlich, *Polymer Chemistry*, 2018, **9**, 2328–2335.

61 T. Asano, Y. Nakagawa, M. Tamura and K. Tomishige, *Applied Catalysis A: General*, 2020, 117723.

62 R. C. Nelson, B. Baek, P. Ruiz, B. Goundie, A. Brooks, M. C. Wheeler, B. G. Frederick, L. C. Grabow and R. N. Austin, *ACS Catalysis*, 2015, **5**, 6509–6523.

63 A. Mahdavi-Shakib, S. Husremovic, S. Ki, J. Glynn, L. Babb, J. Sempel, I. Stavrinoudis, J.-M. Arce-Ramos, R. Nelson, L. C. Grabow, T. J. Schwartz, B. G. Frederick and R. N. Austin, *Polyhedron*, 2019, **170**, 41–50.

64 T. O. Omotoso, B. Baek, L. C. Grabow and S. P. Crossley, *ChemCatChem*, 2017, **9**, 2642–2651.

65 H. Duan, J.-C. Liu, M. Xu, Y. Zhao, X.-L. Ma, J. Dong, X. Zheng, J. Zheng, C. S. Allen, M. Danaie, Y.-K. Peng, T. Issariyakul, D. Chen, A. I. Kirkland, J.-C. Buffet, J. Li, S. C. E. Tsang and D. O'Hare, *Nature Catalysis*, 2019, **2**, 1078–1087.

66 T. J. Schwartz, *Nature Catalysis*, 2019, **2**, 1060–1061.

67 R. W. Gosselink, S. A. W. Hollak, S.-W. Chang, J. van Haveren, K. P. de Jong, J. H. Bitter and D. S. van Es, *ChemSusChem*, 2013, **6**, 1576–1594.

68 B. Peng, Y. Yao, C. Zhao and J. A. Lercher, *Angewandte Chemie International Edition*, 2012, **51**, 2072–2075.

69 T. W. Walker, A. K. Chew, H. Li, B. Demir, Z. C. Zhang, G. W. Huber, R. C. Van Lehn and J. A. Dumesic, *Energy & Environ-*

mental Science, 2018, **11**, 617–628.

70 M. A. Mellmer, C. Sanpitakseree, B. Demir, P. Bai, K. Ma, M. Neurock and J. A. Dumesic, *Nature Catalysis*, 2018, **1**, 199–207.

71 T. J. Schwartz and J. Q. Bond, *Chem. Commun.*, 2017.

72 D. Hibbitts, Q. Tan and M. Neurock, *Journal of Catalysis*, 2014, **315**, 48–58.

73 A. V. H. Soares, J. B. Salazar, D. D. Falcone, F. A. Vasconcellos, R. J. Davis and F. B. Passos, *Journal of Molecular Catalysis A: Chemical*, 2016, **415**, 27–36.

74 K. Makiguchi, T. Satoh and T. Kauchi, *Macromolecules*, 2011, **44**, 1999–2005.

75 C. K. Williams, *Chemical Society Reviews*, 2007, **36**, 1573–1580.

76 J. Zhao and N. Hadjichristidis, *Polymer Chemistry*, 2015, **6**, 2659–2668.

77 A. E. Neitzel, T. J. Haversang and M. A. Hillmyer, *Industrial & Engineering Chemistry Research*, 2016, **55**, 11747–11755.

78 R. C. Pratt, B. G. G. Lohmeijer, D. A. Long, R. M. Waymouth and J. L. Hedrick, *Journal of the American Chemical Society*, 2006, **128**, 4556–4557.

79 L. Simón and J. M. Goodman, *The Journal of Organic Chemistry*, 2007, **72**, 9656–9662.

80 N. Kasyapi and A. K. Bhowmick, *RSC Advances*, 2014, **4**, 27439–27451.

81 M. Aubin and R. E. Prud'homme, *Polymer*, 1981, **22**, 1223–1226.

82 H. Yang, J. Ge, W. Huang, X. Xue, J. Chen, B. Jiang and G. Zhang, *RSC Advances*, 2014, **4**, 23377–23381.

83 M. T. Martello, A. Burns and M. A. Hillmyer, *ACS Macro Letters*, 2012, **1**, 131–135.

84 Y. Shi, X. Cao, S. Luo, X. Wang, R. W. Graff, D. Hu, R. Guo and H. Gao, *Macromolecules*, 2016, **49**, 44166–4422.

85 P. Olsén, K. Odelius and A.-C. Albertsson, *Biomacromolecules*, 2016, **17**, 699–709.